Modeling of the Cloud Interconnected Human Friendly Multi-Agent Based Sustainable Power Controller

G. Gricius, D. Drungilas, J. Guseinovaitė, K. Grigaitis and A. A. Bielskis

***Abstract*-- The paper presents model of the cloud interconnected multi-agent human friendly sustainable power controller (Controller). The Controller is based on the human ambient comfort affect reward index (ACAR index). The ACAR index depends on human physiological parameters: the temperature, the ECG- electrocardiogram and the EDA-electro-dermal activity. These physiological parameters are used for sustainable power control by multi-agent system developed as the cloud interconnected, instrumented, and intelligent environment. The Environment Sense Agent, the Environment Adaptation Agent, the Raw Data Processing and EDA Parameters Extraction Agent, and the Neural Network Training Agent are proposed and implemented into the multi-agent based emotion recognition and environment control system. The modeling results show that proposed system can find such the environmental state characteristics that may improve comfort for people affected by this environment.**

Index Terms—**Multi-agent power controller, cloud computing, emotion recognition, smart environment**

I. Introduction

THE investigation of dynamic interrelation between mind and body dates back to the beginning of 20th century. However, the connection between specific somatic states and different emotions is still a very promising field for investigations. Emotion recognition is achieved by multiple methods. One of the ways is through use of biosensors, which are claimed to be more advantageous than other methods by being unobtrusive and resistant to different environmental conditions [1]. There were attempts to value emotion-induced physiological state by measuring cardiorespiratory (ECG and respiratory) activity. However, the study indicated the need to better define all the factors involved in cardio-respiratory regulation during emotion [2]. Another way is based on measuring human skin resistance. There is constructed an ESI (emotional stress indicator) kit, which captures the changes in human skin resistance and based on that measures the person's stress level [3]. According to galvanic skin response theory, resistance varies inversely proportional to the stress. The lowering of skin resistance during stress is caused by an increased blood flow and permeability, which increases the electrical conductivity of the skin. The same principle is used in a lie detector or psychogalvanometer. It is worth mentioning that there are certain diseases which can affect the skin resistance pattern and that should be considered while interpreting the data [4]. The third major criteria are the change in body temperature. Literature presents some data claiming that anger causes a sharp increase in body temperature, and fear is marked by an opposite response. [5]

The European Union has actively promoted political campaigns toward energy efficiency and renewable energy [6]. The model of Home/Building Automation system [7] to control rolling shutters, heat pump and lighting system finalized to users comfort and energy saving, maximizing the exploitation of solar energy [8]. Multi-Agent Based E-Social Care Support System for Inhabitancies of a Smart Eco-Social Apartment is proposed in [9].This system was developed as an Ambient Comfort Affect Reward Based Multi-Agent Lighting Controller in [11]. The variable air volume (VAV) type of heating, ventilating, and/or air-conditioning (HVAC) systems can be controlled by using simple ON-OFF, intelligent ON-OFF and optimal Controllers [12]. Reinforcement Learning [13] for Building Environmental Control[14] helps to creating of users thermal and lighting comfort in the sustainable home. LED lighting can also increase comfort and save energy in the sustainable home. Nevertheless, according to Directive 2006/25/EC [8], the artificial optical radiation (AOR) exposure leads to health effects for specific wavelength and energy absorbed by different anatomical structures such as skin and eyes. The evaluation of exposure to AOR involves the wavelength classification in ranges between: 180 nm and 400 nm, due to photochemical retinal damage, skin rash, elastosis and skin cancer; 300 nm and 600 nm (blue light), due to photochemical retinal damage; 380 nm and 1400 nm (visible light and infrared), due to thermal retinal damage [10]. Our eyes need light to work, but too much of the wrong kind of light can lead to diseases like age-related macular degeneration, and there is more evidence that blue light (400 –

This work was partly supported by project "Promotion of Student Scientific Activities" (VP1-3.1-ŠMM-01-V-02-003) from the Research Council of Lithuania (K. G.). This project is funded by the Republic of Lithuania and European Social Fund under the 2007-2013 Human Resources Development Operational Programme's priority 3.

G. Gricius is with the Department of Electrical Engineering of Klaipeda University, Klaipeda, 92294 Lithuania (e-mail: gediminas@ik.ku.lt).

D. Drungilas is with the Department of Electrical Engineering of Klaipeda University, Klaipeda, 92294 Lithuania (e-mail: dorition@gmail.com).

J.Guseinovaitė is with Faculty of Medicine of Vilnius University, Vilnius, 03101 Lithuania (e-mail: jurgita.guseinovaite@gmail.com)

K. Grigaitis is with Faculty of Medicine of Vilnius University, Vilnius, 03101 Lithuania (e-mail: grigaitis.kazimieras@yahoo.com)

A.A.Bielskis is with the Department of Electrical Engineering of Klaipeda University, Klaipeda, 92294 Lithuania (e-mail: andrius.bielskis@ik.ku.lt).

500nm) can damage our eyes, with people who have had cataracts removed being particularly vulnerable [7]. Infrared and ultraviolet LEDs can also be hazardous [15]. Principles of development of the model of the Cloud Interconnected Human Friendly Multi-Agent Based Sustainable Power Controller are described in this paper.

II. The Ambient Comfort Affect Reward Based Sustainable Power CONTROLLER MODEL

The model of multi-agent ambient comfort affect reward based sustainable power controller system of Fig. 1 consists of the following parts: the *Environment Evaluation Intelligent Service*, the radial basis neural network, *the RBF Intelligent Service*, and the *Learning Algorithm* service. The *Environment Evaluation Intelligent Service* is used to evaluate the ambient human comfort by sensing the affect of the following environment parameters: the temperature, the lighting, and the air conditioning.

The human comfort is expressed as an Ambient Comfort Affect Reward, the *ACAR*, index function:

$$ACAR = f\{a(l_{ci}, t_a, a_{ci}, t_b, c, d), v(l_{ci}, t_a, a_{ci}, t_b, c, d)\},$$
$$ACAR = [-3,3], \quad (1)$$

where a and v are arousal and valence functions respectively dependent on the following ambient comfort and human physiological parameters: l_{ci} – the modified color lighting index from [2] for local dimmable RGBY LEDs in the laboratory, $T_z = t_a$ – ambient temperature of the zone, $Wz = a_{ci}$ – air conditioning index of specific humidity in the zone, t_b – human body temperature, c – *ECG*, electrocardiogram and d – *EDA*, electro-dermal activity. The (1) type function can be approximated by neural networks, fuzzy logic or other regression methods. In this case, we use fuzzy logic to approximate (1) by defining two fuzzy inference systems: the *Arousal-Valence System*, and the *Ambient Comfort Affect Reward (ACAR) System*. (See Fig.2)

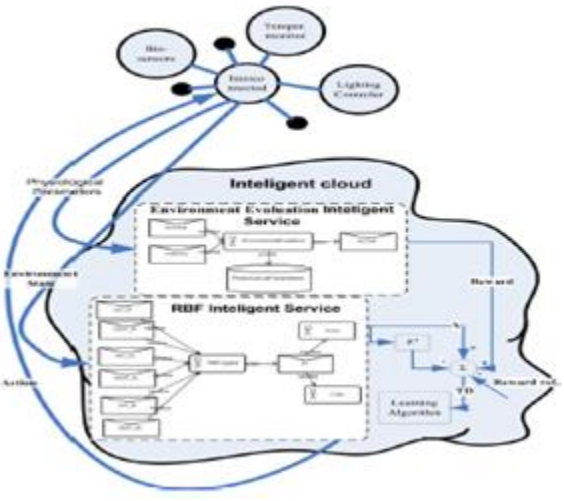

Fig.1. Block diagram of the Ambient Comfort Affect Reward Based Sustainable Power Controller system

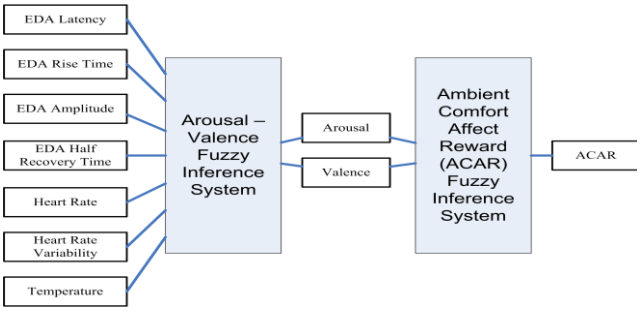

Fig.2. Ambient Comfort Affect Reward (ACAR) System

III. Scenario Monitoring Agents

The *Environment Evaluation Intelligent Service* of Fig.1 is implemented by introducing the following scenario monitoring agents: the Environment Sence Agent and the Environment adaptation agent.

A. Environment Sense Agent

The *Environment Sence Agent* is discribed by pseudo-code of Fig.3. It uses the measured *Temperature raw data*, *Lighting raw data*, and *Air quality raw data* as the input parameters. The agent's output is the following ambient environment parameters: *temperature*, *temperature change*, *lighting*, *lighting change*, *air quality*, and *air quality change*.

Input: *Temperature raw data*
Lighting raw data
Air quality raw data
Output: *Environment = {temperature, temperature change, lighting, lighting change, air quality, air quality change}*
// ambient environment parameters
Initialize: *sampling time T*
WHILE *not end of signal* **DO**
t = sample Temperature raw data at time τ
l = sample Lighting raw data at time τ
a = sample Air quality raw data at time τ
$\Delta t = t_k - t_{k-1}$ *//temperature change*
$\Delta l = l_k - l_{k-1}$ *//lighting change*
$\Delta a = a_k - a_{k-1}$ *//air quality change*
Environment={t, l, a, Δt, Δl, Δa}
ENDWHILE

Fig.3. Pseudo-code fragment for describing of the *Environment Sense Agent*

B. Environment Adaptation Agent

Fig.4 depicts a pseudo-code fragment of the *Environment Adaptation Agent.* The Agent takes the *initial environment state* as an input and gives the following output parameters: *State trace*, *Action trace*, *Temporal difference trace*, and *Value trace*.

IV. Measured Emotional Data Preprocessing Agents

The *RBF Intelligent Service* of Fig.1 is implemented by introducing the following measured emotional data preprocessing agents: the *Raw Data Preprocessing and EDA Parameters Extraction Agen*t and the *Neural Network Training Agent.*

A. Raw Data Processing and EDA Parameters Extraction Agent

Fig.5 depicts a pseudo-code fragment of the *Environment Adaptation Agent.* The Agent takes the following input parameters: *raw data of EDA measurements, X, sampling time of X, class indicator of emotional state, S,* and *sampling time of S.* The output of the Agent predicts the EDA parameters: *latency, EDA rise time, EDA ampliude*, and *EDA half recoveery time*.

Input: $state_{t=0}$ // *the initial environment state*
Output: state trace
Action trace
Temporal difference trace
Value trace
Initialize: $\Delta reward$ // *the change of the reward*
$ARVA_{t=0}$ // *the initial arousal-valence value vector*
$ACAR_{t=0}$ // *the Ambient Comfort Affect Reward*
center // *the centers of basis functions*
σ // *the width of basis functions*
γ // *the discount factor*
λ // *the decay factor*
$e_{t=0}=0$ // *the eligibility trace*
α // *the learning rate*
v // *the RBF neural network weights of actor*
w // *the RBF neural network weights of critic*
FOR *each* t^{th} *observation* **DO**
FOR *each action* **DO**
Initialize: $V_j=0$
FOR *each* j^{th} *basis function center* **DO**

$$\phi_j^{critic} = \exp\left(-\frac{\left\|state_t - center_j\right\|^2}{2\sigma_j^2}\right)$$

$V_j=V_j+ \Phi_j^{\text{critic}} \cdot w_j$
ENDFOR
$e_{t+1}=\gamma \cdot \lambda \cdot e_t+ \Phi_j^{\text{critic}}$
$\delta_t= ACAR_t + V_{j-1} - \gamma \cdot V_j$ // *the temporal difference*
FOR *each basis function center j* **DO**
$w_j = w_j + \alpha \cdot \delta_t \cdot e_{t+1} \cdot \Delta reward$
ENDFOR
Initialize: $action_t=0$
FOR *each basis function center j* **DO**
$v_j= v_j + \alpha \cdot \delta_t \cdot e_{t+1} \cdot \Delta reward$

$$\phi_j^{actor} = \exp\left(-\frac{\left\|state_t - center_j\right\|^2}{2\sigma_j^2}\right)$$

$action_t= action_t + \Phi_j^{\text{actor}} \cdot v_j;$
ENDFOR
get new state: $state_{t+1} = state_t + action_t$
simulate Arousal Valence: $ARVA_{t+1} = FIS(state_{t+1})$
// *FIS – Fuzzy Inference System*
$ACAR_{t+1} = FIS(ARVA_{t+1});$
$\Delta Reward = ACAR_{t+1} - ACAR_t$
ENDFOR
ENDFOR

Fig.4. Pseudo-code fragment of the *Environment Adaptation Agent*

Input: $X = x_1, x_2, \ldots, x_n$ // *raw data of EDA measurements, X*
$Tx = tx_1, tx_2, \ldots, tx_n$ // *sampling time of X*
$S = s_1, s_2, \ldots, s_i$// *class indicator of emotional state, S*
$Ts = ts_1, ts_2, \ldots, ts_i$ //*sampling time of S*
Output: EDA parameters
Initialize: $L = l_1, l_2, \ldots, l_i$ // *latency*
$RT = rt_1, rt_2, \ldots, rt_i$ // *EDA rise time*
$A = a_1, a_2, \ldots, a_i$ // *EDA amplitude*
$HRT = hrt_1, hrt_2, \ldots, hrt_i$// *EDA half recovery time*
X=**ksmooth(**X**)** //*kernel regression smoothing*
$j=1$
FOR *each* s_k **DO**
WHILE $tx_j<ts_k$ **DO** //*looking for beginning of stimulus*
$j=j+1$
ENDWHILE
$Xstart= tx_j$
$Ystart= x_j$
WHILE $x_j>= x_{j+1}$ **DO** //*looking for beginning of EDA rising*
$j=j+1$
ENDWHILE
$l_k= tx_j - Xstart$ //*calculating the latency*
$Xstart= tx_j$
WHILE $x_j<x_{j+1}$ **DO** //*looking for EDA peak*
$j=j+1$
ENDWHILE
$rt_k = tx_j - Xstart$ //*calculating the rise time*
$Xstart= tx_j$
$a_k = x_j - Ystart$ //*calculating the amplitude*
$Ystart= x_j$
WHILE Ystart - $x_j< a_k/2$ **DO**//*looking for EDA half recovery*
$j=j+1$
ENDWHILE
$hrt_k = tx_j - Xstart$// *calculating the half recovery time*
ENDFOR

Fig.5. Pseudo-code fragment of the *Raw Data Preprocessing and EDA Parameters Extraction Agen*t.

B. Neural Network Training Agent

Fig.6 presents a pseudo-code fragment of the *Neural Network Training Agent.* The Agent takes the following as an Input: *Pattern= {L, RT, A, HRT}* and *Class={S}.*The output of this agent is the *trained neural network, NN.*

Input: *Pattern={L, RT, A, HRT}*
Class={S}
Output: *NN // trained neural network*
Initialize: *NN //initial neural network with 4 inputs 8 outputs*
W //initial random neural network weights
FOR *each iteration t* **DO**
FOR *each example n* **DO**
run Patern forward through network, computing all o_i *(outputs of NN nodes) and* in_i *(inputs for hidden layers) for all weights (j,i)*
$\Delta_i= (Class_i-a_i)\cdot g'(in_i)$ // *weight correction if i is output node*
$\Delta_i= g'(in_i)\Sigma_k w_{ik}\Delta_k$ // *weight correction if i is not output node*
$w_{ji} = w_{ji}+\alpha\cdot a_j\cdot\Delta_i$ // *update NN weights*
ENDFOR
ENDFOR

Fig.6. Pseudo-code fragment of the *Neural Network Training Agen*t.

V. PRACTICAL IMPLEMENTATION OF ELEMENTS OF SUSTAINABLE POWER CONTROLLER FOR THE SINGLE ROOM LABORATORY

Fig. 7 represents the following wireless communication elements of prototype of the ACAR-Controller for the single room laboratory: The block diagram of the sustainable electric power distribution subsystem for measuring, sustainable control and delivering power to electric heater and fans by

using triac type AC power controllers DIM1 and DIM2 driven by MEGA32 type boards of Fig. 7a; The block diagram of the intelligent RGBY lighting subsystem, the IRGBY Light, with dimmable current stabilizers for each RGBY power LED to predicting limits of exposure to broad-band incoherent optical radiation by [15] of Fig.7b; The schematic diagram of the Mega128RFA1 transceiver board of Fig.7c. Fig.8 shows the noninvasive measuring subsystem of human reaction to comfort conditions in the laboratory. The ATMEGA128RFA1-ZU transceivers of Fig.7c are used to creating of the wireless communication subsystem between MEGA32 type boards and central computer connected to the Internet. It uses the 802.15.4 ZigBee low-power, short-distance wireless ISM standard for the 2.4GHz license-free radio bands.

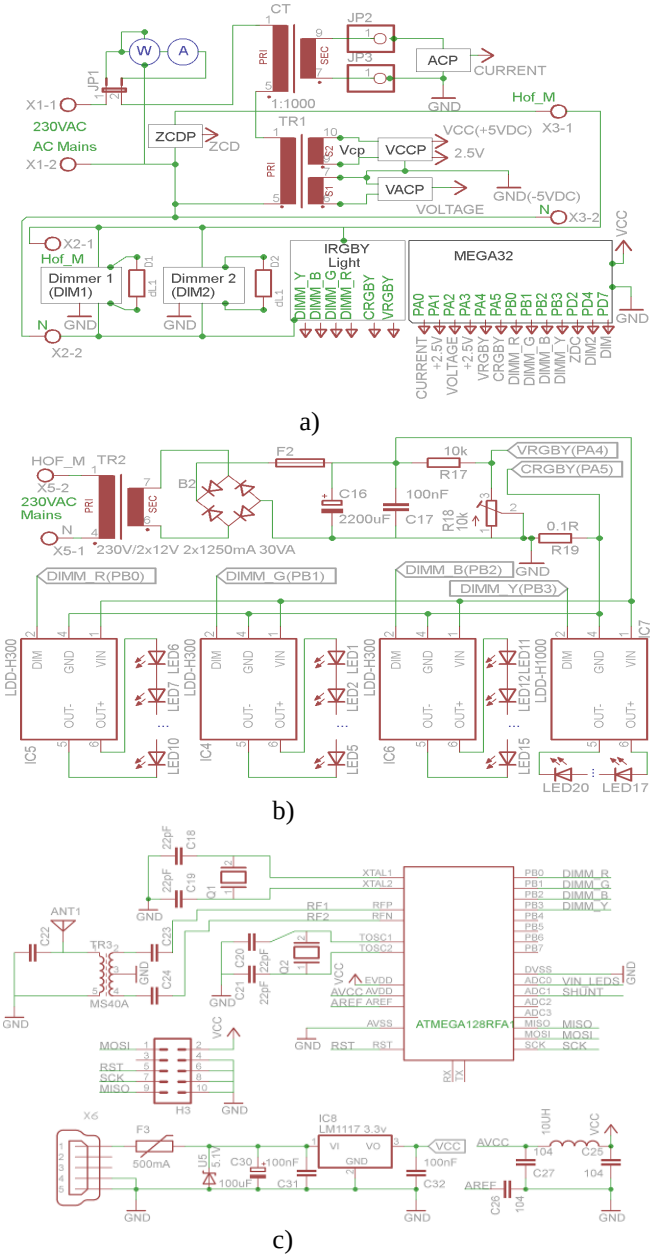

Fig.7. The sustainable electric power distribution subsystem for measuring, sustainable control and delivering power to electric heater and fans by using triac type AC power controllers driven by MEGA32 type boards: a) block diagram; b) IRGBY Light - the intelligent RGBY lighting subsystem with dimmable current stabilizers for each RGBY power LED; c) Mega128RFA1 transceiver board.

The subsystem for non-invasive measurements of human physiological parameters: the body temperature, the ECG-electrocardiogram and the EDA-electro-dermal activity to predicting human reaction to comfort conditions in the laboratory is presented in Fig.8. Fig.9 represents C program block for implementation of digital measurements of output signals of *VOLTAGE* (*VACP* block of Fig. 7a) and *CURRENT* (*ACP* block of Fig. 7a) by MEGA32 type board.

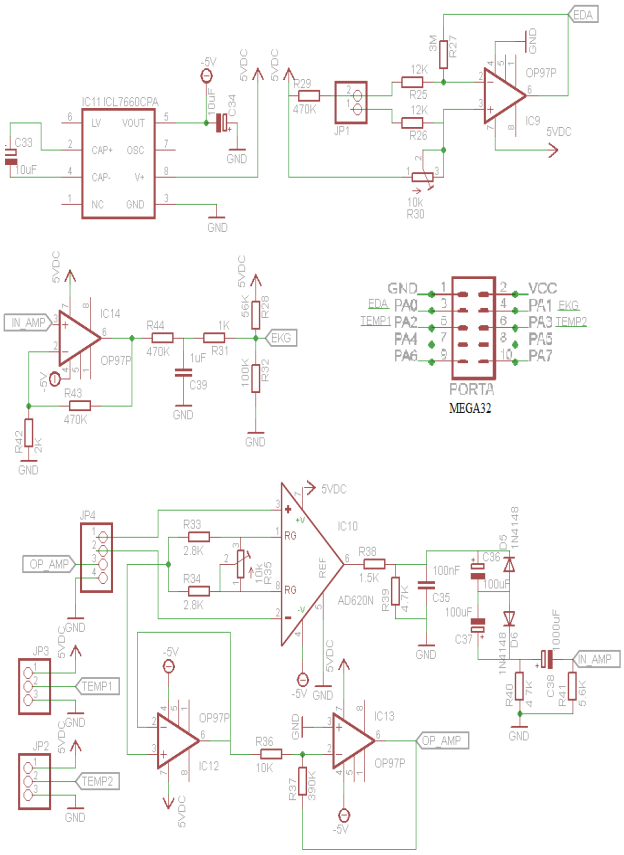

Fig.8. Schematic diagram of experimental subsystem for non-invasive measurements of human physiological parameters: the body temperature, the ECG-electrocardiogram and the EDA-electro-dermal activity to predicting human reaction to comfort conditions in the laboratory.

```
msr_info.v_rms_sum        +=        (int32_t)msr_info.
raw_inst_voltage *  msr_info.raw_inst_voltage;
msr_info.i_rms_sum        +=        (uint32_t)msr_info.
raw_inst_current * msr_info.raw_inst_current;
msr_info.vi_sum     +=     (int32_t)msr_info.raw_inst_
voltage*msr_info.raw_inst_current
double   v_rms   =   sqrt((double)msr_info.v_rms_sum   /
NUM_SAMPLES * v_coef * v_coef);
double   i_rms   =   sqrt(((double)msr_info.i_rms_sum   *
pow(i_coef/gain, 2)) / NUM_SAMPLES);
double p = (int32_t)msr_info.vi_sum / NUM_SAMPLES *
(i_coef/gain) * v_coef;
```

Fig.9. C program block for implementation of digital measurements of output signals of *VOLTAGE* (*VACP* block of Fig. 7a) and *CURRENT* (*ACP* block of Fig. 7a) by MEGA32 type board

VI. Results and Discussion

Fig. 10 represents digital measurement results of instantaneous values of 50 Hz mains voltage, *u* (V), taken as the output signals, *VOLTAGE*, of the *VACP* block of Fig. 7a and the mains instantaneous current, *i* (mA), taken as the output signals, *CURRENT*, of the *ACP* block of Fig. 7a versus time (sec*10^{-3}) measured by MEGA32 type board and calculated by the program of *Atmega Oscilloscope* respectively: for voltage, *u* (V), a) and current *i* (mA), b) of 0,7 kW heater, for voltage, *u* (V), c) and current *i* (mA), d) of the computer monitor, and for voltage, *u* (V), e) and current *i* (mA), f) of an refrigerator. Fig.11 depicts the screen shots of *Atmega Oscilloscope* program of instantaneous mains current, *i* (mA), versus time in sec*10^{-3} for: a) Unregulated 100W bulb; b) 100W bulb, regulated angle, α= 45°; c) 100W bulb, regulated angle, α= 45°, filtering: choke; d) 100W bulb, regulated angle, α= 45°, filtering: capacitor; e) 100W bulb , regulated angle, α= 45°, filtering: choke and capacitor. The current, *i* (mA), trough the 100W bulb type load was dimmed by triac type dimmer, *DIM1*, and measured by using the *CURRET* as an output signal of *ACP* block of Fig.7a.

The calculations of RMS values of current, $I_{RMS} = SQRT((\Sigma(v_iC_i/G)^2/n)$ = 2825.6 mA , voltage, $V_{RMS} = SQRT((\Sigma(v_vC_v)^2/n) = 230.0\ V$, apparent power, $S_{appparent} = V_{RMS}*I_{RMS}$ = 649.9 VA, active power, $P = \Sigma(v_iC_iv_vC_v/nG)$ = 628.119 W, power factor, $PF = P/S_{appparent}$ = 0.9665, C_i = 0.1206, C_v = 0.75, G = 1|10|200, and n = 3000 for the 0,7 kW heater are performed by system software every 0.7 sec. The constants C_v and C_i were calculated by using values of voltmeter, *V*, amp meter, *A*, and watt meter, *W*, of Fig.7a. The values of power factor of monitor and refrigerator are as follows: $PF_{monitor}$ = 0.3437 and $PF_{refrigarator}$ = 0.2598.

Digital measurements of instantaneous values of *k* sample of the mains voltage $(v_k + v_{k+2})/2$ and current i_{k+1} taken by the load from the mains have been performed every 0.8 sec*10^{-3} at 25 samples per 20 sec*10^{-3} period or 14.4°. Instantaneous active power value $p_k = ((v_k + v_{k+2})/2)* i_{k+1}$ was calculated after 3 first type differential convertions of every adjasent sample that takes 25 ADC clock cycles at a maximum speed of convertion of 200 KHz each, and 25/200.10^3 = 0.125 sec*10^{-3} or 6.28*0.125/20=0.03925 radians/2.25 degrees.

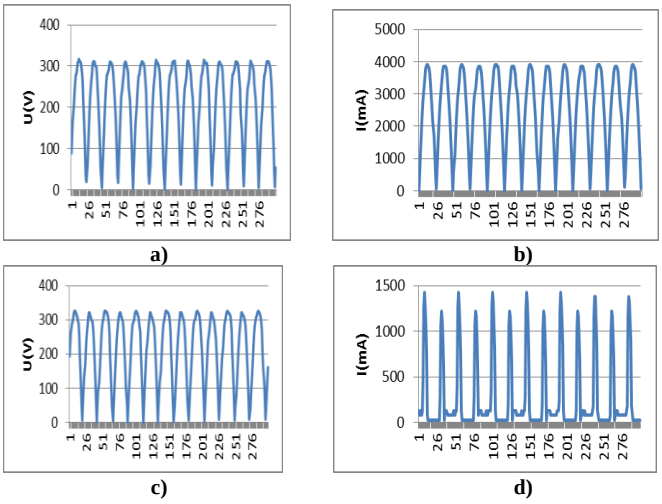

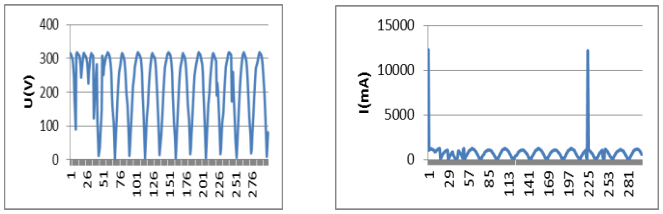

Fig.10. Screen shots of the program *Atmega Oscilloscope* of instantaneous values of output signals of *VOLTAGE* and *CURRENT* versus time in sec*10^{-3} measured by MEGA32 type board of Fig.2a respectively: for voltage, a) and current, b) of 0,7 kW heater; for voltage, c) and current, d) of computer monitor; for voltage, e) and current, f) of refrigerator.

The sample error can be: between the values of Err_{max}=512*(*sin*(0.03925)=20,09 (3.92%) and Err_{min}=512* *sin*(3.14/2) - (3.14/2-0.03925))=0.461(0.09%) which is acceptable.

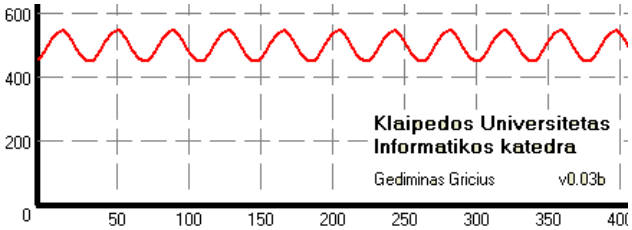

a) Unregulated 100W bulb, U_{RMS}=232 V, I_{RMS}=443 mA, Apparent power: 102,09 VA, Active power: 100,68 W, Power factor: 0,986

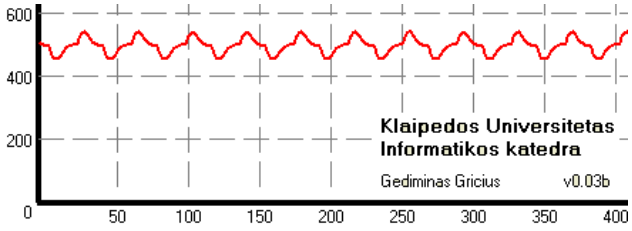

b) 100W bulb, α= 45°, U_{RMS}=232 V, I_{RMS}=318 mA, Apparent power: 73,79 VA, Active power: 36,60 W, Power factor: 0,496;

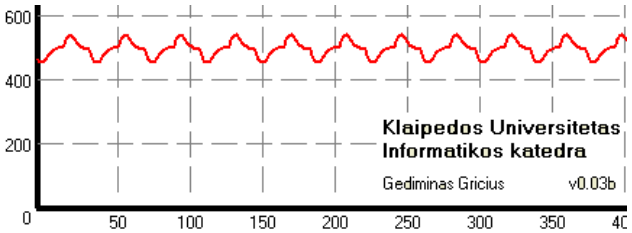

c) 100W bulb, α= 45°, filtering: choke, U_{RMS}=232 V, I_{RMS}=319 mA Apparent power: 73,18 VA Active power: 36,72 W Power factor: 0.502;

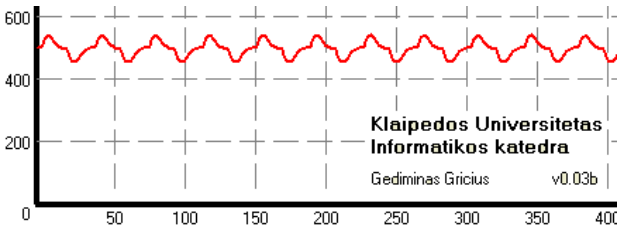

d) 100W bulb, α= 45°, filtering: capacitor, U_{RMS}=231 V, I_{RMS}=314 mA, Apparent power: 72,63 VA, Active power: 35,53 W, Power factor: 0,489;

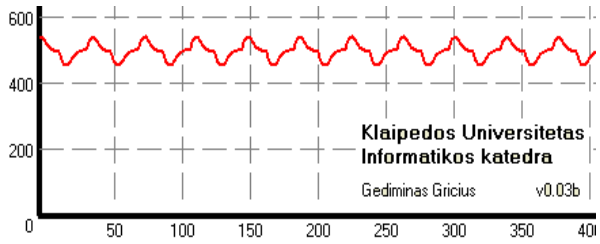

e) 100W bulb , α= 45°, filtering: choke and capacitor, U_{RMS}=231 V, I_{RMS}=314 mA, Apparent power: 72,94 VA, Active power: 35,88 W, Power factor: 0,492

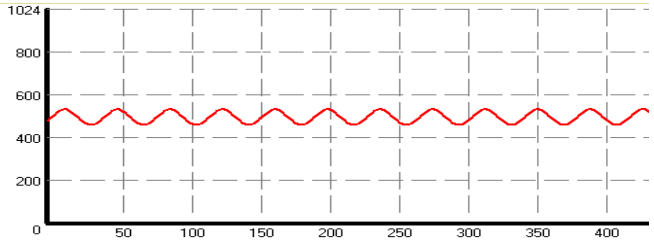

f) **Fan,** U_{RMS}=230 V, I_{RMS}=330 mA, Apparent power: 75.90 VA, Active power: 51.87 W, Power factor: 0.68

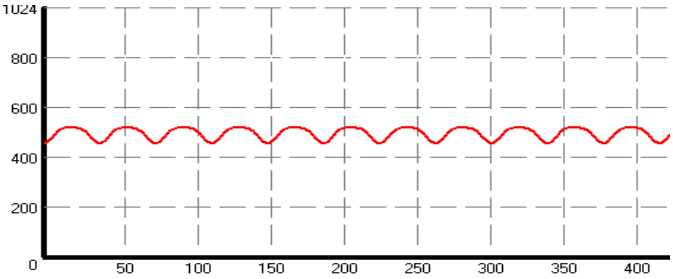

g) **Fan, , α= 5°,** U_{RMS}=230 V, I_{RMS}=288 mA, Apparent power: 66.24 VA, Active power: 46.43 W, Power factor: 0.70

Fig.11. Screen shots of *Atmega Oscilloscope* program of instantaneous current in mA versus time in 10^{-3}*sec for: a) Unregulated 100W bulb; b) 100W bulb, α= 45°; c) 100W bulb, α= 45°, filtering: choke; d) 100W bulb, α= 45°, filtering: capacitor; e) 100W bulb , α= 45°, filtering: choke and capacitor; f) Unregulated fan; g) Dimmable fan, α= 5°.

The measurement results of Fig.6 illustrate how dimming and filtering influence the parameters of power distributed to feeding the incandescent lamp of 100 W. For the case of Fig.11a of unregulated 100 W bulb**,** we have U_{RMS}=232 V, I_{RMS}=443 mA, apparent power, $S_{appparent}$ = 102,09 VA, active power, P = 100,68 W, power factor= 0,986. For Fig.11b of 100 W bulb with regulated angle, α=45°, we have U_{RMS}=232 V, I_{RMS}=318 mA, apparent power, $S_{appparent}$ = 73,79 VA, active power, P = 73,68 W, power factor= 0,496. For Fig.11c of 100 W bulb with regulated angle, α=45°, and filtering in series with 100 μH choke**,** we have U_{RMS}=232 V, I_{RMS}=319 mA, apparent power, $S_{appparent}$ = 73,18 VA, active power, P = 36,72 W, power factor= 0,502. For Fig.11d of 100 W bulb with regulated angle, α=45°, and filtering in parallel to the load with 470 nF capacitor**,** we have U_{RMS}=231 V, I_{RMS}=314 mA, apparent power, $S_{appparent}$ = 72,63 VA, active power, P = 35,53 W, power factor= 0,489. For Fig.11e of 100 W bulb with regulated angle, α=45°, filtering in series with 100 μH choke and in parallel to the load with 470 nF capacitor**,** we have U_{RMS}=231 V, I_{RMS}=314 mA, apparent power, $S_{appparent}$ = 72,94 VA, active power, P = 35,88 W, power factor= 0,492.

The dimming process introduces reactive power even in that case when there is an active load. It is seen from the results of Fig.6b where feeding the 100 W bulb with regulated angle, α=45°, we obtain the power factor= 0,496.

The simistor (triac) type dimmer introduces feature of capacitor type load and its influence may be minimized by introducing inductance type filter connected in series with the load. This statement can be proved by Fig.11c where 100 W bulb with regulated angle, α=45°, and filtering in series with 100 μH choke has the power factor= 0,502. The statement also can be proved by using Fig.11d where the power factor= 0,489 decreased when the 100 W bulb is fed from the 50 Hz mains with regulated angle, α=45°, and filtering in parallel to the load with 470 nF capacitor. The Fig. 11e demonstrates that filtering the load of 100 W bulb with regulated angle, α=45°, by using 2nd order filter in series with 100 μH choke and in parallel to the load with 470 nF capacitor does not make sense because in this case the power factor= 0,492, and it is less then in the case of Fig.11c when only filtering in series with 100 μH choke was used.

If the current, *i* (mA), trough the 75 VA single phase motor of the fan was dimmed by triac type dimmer, *DIM2*, and measured by using the *CURRENT* as an output signal of *ACP* block of Fig.7a, the dimming process increases the power factor. It is proved by using screen shots of *Atmega Oscilloscope* program shown in Fig.11f and 6g. Fig.11f gives data for fan fed by single phase 50 Hz mains with U_{RMS}=230 V, $I_{RM\,S}$=330 mA, apparent power=75.90 VA, active power= 51.87 W, power factor=0.68. Fig.11g gives data for dimmable fan with regulated angle, α= 5°, fed by single phase 50 Hz mains with U_{RMS} =230 V, I_{RMS}=288 mA, apparent power = 66.24 VA, active power = 46.43 W, and power factor=0.70.

VII. Conclusions

The model of the Cloud Interconnected Human Friendly Sustainable Power Controller is proposed based on describing of the Environment Evaluation Service, the Radial Basis Neural Network Service, and the Learning Algorithm Service in the multi-agent approach.

The Controller is based on the human ambient comfort affect reward index (ACAR index) which depends both on human physiological parameters: the temperature, the ECG-electrocardiogram and the EDA-electro-dermal activity as well as on the parameters of the sustainable electric power distribution subsystems for measuring, control and delivering power to electric heater, fans, and the intelligent RGBY LED lighting in a single room laboratory by using triac type AC power controllers driven by MEGA32 type boards.

The ATMEGA128RFA1-ZU transceivers are used to creating the cloud interconnected, instrumented, and intelligent environment by using MEGA32 type boards and central computer connected to the Internet.

The pseudo-codes of the Environment Sense Agent, the Environment Adaptation Agent, the Raw Data Processing

and EDA Parameters Extraction Agent, and the Neural Network Training Agent are proposed and implemented into the multi-agent based emotion recognition and environment control subsystem.

The modeling results show that the proposed system is able to automatically find such the environmental state characteristics that can improve both the power characteristics as well as the comfort conditions for people affected by this environment in the single room laboratory.

VIII. Acknowledgment

The authors gratefully acknowledge Lithuania Research Council for support of Project „Promotion of Students' Scientific Activities": http://studentai.lmt.lt/DOKUMENTAI/REZULTATAI/smp_2012_fbtz_finansuojamipt.pdf and the contributions of prof. E. Guseinovienė for her work on the original version of this document.

References

[1] A. Haag, S. Goronzy, P. Schaich, J. Williams, "Emotion Recognition Using Bio-sensors: First Steps towards an Automatic System", *Affective Dialogue Systems Lecture Notes in Computer Science*, Vol. 3068, 2004, pp.36-48.

[2] P. Rainville, A. Bechara, N. Naqvi, A.R. Damasio, "Basic emotions are associated with distinct patterns of cardiorespiratory activity", *International Journal of Psychophysiology*, Vol.61, No.1, July 2006, pp.5-18.

[3] A.A. Abdullah, U.H. Hassan, "Design and development of an emotional stress indicator (ESI) kit", *Sustainable Utilization and Development in Engineering and Technology (STUDENT)*, 2012 IEEE Conference, 6-9 October 2012, pp.253-257.

[4] P. Mika, Anu S. Tarvainen, Koistinen, Minna Valkonen-Korhonen, Juhani Partanen and Pasi A. Karjalainen, "Analysis of Galvanic Skin Responses With Principal Components and Clustering Techniques", *IEEE Transactions on Biomedical Engineering*, Vol.48, No.10, October 2001, pp.1071-1079.

[5] Philippot, P., Rimé, B., The perception of bodily sensations during emotion: A cross-cultural perspective", *Polish Psychological Bulletin*, 1997, 28, pp.175-188.

[6] G. Zheng, Y. Jing, H. Huang, P. Ma,"Thermal Comfort and Indoor Air Quality of Task Ambient Air Conditioning in Modern Office Buildings," *International Conference on Information Management, Innovation Management and Industrial Engineering, ICIII '09 Proc. 2009*, Vol.2, pp.533-536.

[7] S.M. Zanoli, D. Barchiesi, "Thermal and Lighting Control System with Energy Saving and Users Comfort Features", *Proc. 2012 IEEE 20th Mediterranean Conference on Control & Automation (MED)* Barcelona, pp.1322-1327.

[8] DIRECTIVE 2006/25/EC of the European Parliament and of the Council of 5 April 2006 on the minimum health and safety requirements regarding the exposure of workers to risks arising from physical agents (artificial optical radiation), 19th individual Directive within the meaning of Article 16(1) of Directive 89/391/EEC.

[9] Quarto, A., Di Lecce, V., Dario, R., Uva, J.**,** "Personal dosimeter for the measurement of artificial optical radiation (AOR) exposure", *Proc. IEEE International Conference on Computational Intelligence for Measurement Systems and Applications (CIMSA)*,2011, pp.1-6.

[10] A.A. Bielskis, A. Andziulis, O. Ramašauskas, E. Guseinovienė, D. Dzemydienė, G. Gricius, **"**Multi-Agent Based E-Social Care Support System for Inhabitancies of a Smart Eco-Social Apartment", *Electronics and Electrical Engineering*, 2011, Vol.1-(107), pp.11–14.

[11] A.A. Bielskis, E. Guseinovienė, D. Dzemydienė, D. Drungilas, G. Gricius, "Ambient Lighting Controller Based on Reinforcement Learning Components of Multi-Agents", *Electronics and Electrical Engineering*, Vol.5-(121), 2012, pp.79-84.

[12] K. Chinnakani, A. Krishnamurthy, J. Moyne, A. Arbor, and F. Gu, "Comparison of Energy Consumption in HVAC Systems Using Simple ON-OFF, Intelligent ON-OFF and Optimal Controllers", *Proc. IEEE Power and Energy Society General Meeting*, 2011, pp.1-6.

[13] R.S. Sutton, A.G. Barto, Reinforcement learning: An Introduction. Cambridge, MA: MIT Press**,** 2011.

[14] K. Dalamagkidis, D. Kolokotsa, Reinforcement Learning for Building Environmental Control", *Reinforcement Learning: Theory and Applications*, Book edited by Cornelius Weber, Mark Elshaw and Norbert Michael Mayer ISBN 978-3-902613-14-1, I-Tech Education and Publishing, Vienna, Austria, January 2008, pp.424.

[15] *ICNIRP Guidelines on limits of exposure to broad-band incoherent optical radiation (0.38 to 3 microM)*, ICNRP Statement @, 2011

Biographies

Gediminas Gricius is a Ph.D. student at the Department of Software Engineering of Vilnius University Institute of Mathematics and Informatics (Lithuania) and works as an lecturer at the Klaipeda University. He graduated MSc degree in computer science, Klaipeda University in 2010. Research interests include embedded systems, automated control and agent-based modeling.

Darius Drungilas is a PhD student at Institute of Mathematics and Informatics, Vilnius University (Lithuania). He graduated MSc degree in computer science, Klaipeda University in 2009. He is lecturer at the Department of Informatics engineering and Electrical Engineering of the Faculty of Marine Engineering of the Klaipeda University (Lithuania). His research interests include methods of artificial intelligence, agent-based modeling, digital adaptive control, machine learning and data mining.

Jurgita Guseinovaitė (born in 1992) is a 4th year medical student in Faculty of Medicine, Vilnius University. In summer 2013 she took part in summer practice in Klaipeda University Hospital at Oncology Department. Areas of interest include normal and pathological physiology, oncology and oncosurgery.

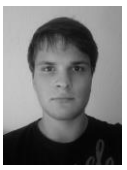

Kazimieras Grigaitis (born in 1991) is a 4th year medical student in Faculty of Medicine, Vilnius University. In summer 2012 he took part in project "Promotion of Student Scientific Activities". In 2013 he participated in summer practice Klaipeda University Hospital at Traumatology Department. Areas of interest include human physiology, biomechanics, orthopaedics and traumatology, surgery.

Antanas Andrius Bielskis is professor, doctor habilitatis of the Informatics, Electrical Engineering Departments of Klaipeda University and of the Department of Informatics of Lithuanian Business University of Applied Sciences He holds the diplomas of radio-engineering in 1959 of Kaunas Institute of Technology, PhD in Electronic Engineering in 1968 of Moscow Institute of Communications, and Doctor of Science in Power Electronics and Communications in 1983 of the Institute of Electrodynamics of Academy of Science of Ukraine.

In 1959-1964, he was the designer, project manager at the Klaipeda Ship Design Institute, in 1964-1990 - senior lecturer, associate professor, head of the departments of Electrical Engineering and Physics - Mathematics, professor of the Klaipeda faculty of the Kaunas Polytechnic Institute (now Kaunas University of Technology), and in 1991 up to now– professor of Klaipeda University.

His research interests include methods of artificial intelligence, knowledge representation techniques, development of smart embedded energy distribution systems.